Hawley's

Condensed Chemical

Dictionary

THIRTEENTH EDITION

Revised by

Richard J. Lewis, Sr.

This text is printed on acid-free paper. ♾

08/04/2008 19:17 FAX

☑ 018/025

contact. TLV:

ticizer for cel-

.

,CH₂OH.
.n water (20 g/
105C (10 mm
gal (20C), refr
solution 4.51.

agent consist-
with diesel oil.

:ong oxidizing

nitrocotton;

.OH

X

>rphous solid
:olution). Con-
₃6, flash p 55F
High-nitrogen
ie; insoluble in
t form (pyrox-
x and acetone

; cotton linters,
nd sulfuric ac-
mperature and
: ratio, widely

lloided flake or
of several vis-
r be dry or wet

and explosion
n wet.
:s, high explo-
, printing ink
coating book-
tanufacture of

nitrocellulose lacquer. See lacquer.

nitrochlorobenzene. Legal label name (Rail) for chloronitrobenzene.

nitrochloroform. See chloropicrin.

***p*-nitro-*o*-chlorophenyl dimethyl thionophosphate.**
See dicapthon.

nitrocobalamin. $C_{62}H_{90}N_{14}O_{16}PCo$. One of the active forms of vitamin B_{12} in which a nitro group is attached to the central cobalt atom.

nitrocotton. See nitrocellulose.

2-nitro-*p*-cresol. (4-methyl-2-nitrophenol).
$NO_2(CH_3)C_6H_3OH$.
Properties: Yellow crystals. D 1.24 (38/4C), mp approximately 35C, bp 234C. Slightly soluble in water; soluble in alcohol and ether. Combustible.
Hazard: Toxic by ingestion, inhalation, and skin absorption.
Use: Intermediate.

nitrodichloro derivative. See the corresponding dichloronitro derivative.

***o*-nitrodiphenyl.**
See *o*-nitrobiphenyl.

***o*-nitrodiphenylamine.** $C_6H_5NHC_6H_4NO_2$.
Properties: Red-brown, crystalline powder. Mp 75–76C. Combustible.
Use: Stabilizer for nitroglycerin; chemical intermediate.

"Nitrodisc" *[Searle].* TM for nitroglycerin transdermal patch system.
Use: Drug administered by transdermal patch.

nitrodracylic acid. See *p*-nitrobenzoic acid.

nitro dye. A dye whose molecules contain the NO_2 chromophore group.

nitroethane.
CAS: 79-24-3. $CH_3CH_2NO_2$. A nitroparaffin.
Properties: Colorless liquid. D 1.052 (20/20C), fp −50C, bp 114C, vap press 15.6 mm Hg (20C), flash p 106F (41C), autoign temp 779F (415C), bulk d 8.75 lb/gal (20C), refr index 1.3917 (20C). Solubility in water 4.5 cc/100 cc (20C); solubility of water in nitroethane 0.9 cc/100 (20C).
Derivation: By reaction of propane with nitric acid under pressure.
Hazard: Moderate fire risk. TLV: 100 ppm in air.
Use: Solvent for nitrocellulose, cellulose acetate, cellulose acetopropionate, cellulose acetobutyrate, vinyl, alkyd and many other resins, waxes, fats, and

dyestuffs; Friedel-Crafts synthesis; propellant research; fuel additive.

2-nitro-2-ethyl-1,3-propanediol.
$CH_2OHC(C_2H_5)NO_2CH_2OH$.
Properties: White, crystalline solid. Mp 56–75C, bp (decomposes) (10 mm Hg), pH 0.1*M* aqueous solution 5.48. Soluble in organic solvents; very soluble in water.
Use: Organic synthesis.

nitrofuran. Any of several synthetic antibacterial drugs used to treat mammary gland infections in cows and to inhibit disease in swine, chickens, etc. Among them are nitrofurazone, furazolidone, nihydrazone, and furaltadone. All of the latter have been found to cause cancer in laboratory animals, and their use has been discontinued.
See furazolidone.

nitrofurantoin. (*N*-(5-nitro-2-furfurylidene)-1-aminohydantoin).
CAS: 67-20-9. $C_8H_6N_4O_5$.
Properties: Yellow, bitter powder; slight odor. Mp (decomposes) 270–272C. Very slightly soluble in alcohol; practically insoluble in ether and water.
Grade: USP.
Use: Medicine (antibacterial).

nitrogen.
CAS: 7727-37-9. N. Gaseous element of atomic number 7 of group VA of the periodic table, aw 14.0067, valences of 1, 2, 3, 4, 5. There are two stable and four radioactive isotopes; the molecular formula is N_2. Second-highest-volume chemical produced in U.S. (1995). In 1995, 68 billion pounds were produced.
Properties: Colorless, diatomic gas; odorless; tasteless; constituting approximately four-fifths of the air. Colorless liquid, chemically unreactive. D 1.251 g/L (0C, 1 atm), d (gas) 0.96737 (air = 1.00), (liquid) 0.804, (solid) 1.0265, fp −210C, bp −195.5C. Slightly soluble in water and alcohol. Noncombustible, an asphyxiant gas. ←—
Derivation: From liquid air by fractional distillation, by reducing ammonia.
Grade: USP, prepurified 99.966% min, extra dry 99.7% min, water pumped 99.6% min.
Use: Production of ammonia, acrylonitrile, nitrates, cyanamide, cyanides, nitrides; manufacture of explosives; inert gas for purging, blanketing, and exerting pressure; electric and electronic industries; in-transit food refrigeration and freeze drying; pressurizing liquid propellants; quick-freezing foods; chilling in aluminum foundries; bright annealing of steel; cryogenic preservation; food antioxidant; source of pressure in oil wells; inflating tires; component of fertilizer mixtures.

nitrogen-15. A stable isotope, with an atomic mass of 15.00011, present in naturally occurring

Endohedral nitride cluster fullerenes
Formation and spectroscopic analysis of $L_{3-x}M_xN@C_{2n}$ ($0 \leq x \leq 3$; $N = 39, 40$)

L. Dunsch*, M. Krause, J. Noack, P. Georgi

Group of Electrochemistry & Conducting Polymers, Leibniz-Institute of Solid State and Materials Research Dresden, D-01107 Dresden; Germany

Abstract

The class of endohedral fullerenes is demonstrated in its large variety by the new type of nitride cluster fullerenes. These endohedral fullerenes were obtained as the most abundant fullerenes in the soot extract. This is reached by the concept of reactive gas atmosphere in arc burning fullerene production. The chemical reactions in the gas atmosphere during the production are described. Different nitride cluster fullerenes were produced with selectivity up to 90% by using reactive gas addition to the cooling gas of the arc burning process. Fullerenes prepared by this method are Sc₃N@C₈₀, Sc₃₋ₓErₓN@C₈₀ (x = 1, 2, 3), ScₓN@Cₙₐ, YₓN@C₈₀, Ho₃N@C₈₀ and Tb₃N@C₈₀.

By studying Vis/NIR spectra, it is demonstrated that nitride cluster fullerenes are generally large band-gap endohedrals. Therefore, the M₃N@C₈₀ structures are very stable and suitable for applications. This stability is caused by a charge transfer from the cluster to the carbon cage and the formation of a M₃N–carbon cage bond as well as covalent metal nitrogen bonds. Infrared spectroscopy of M₃N@C₈₀ was used to study the metal and cage size influence on the structure of the nitride cluster.

© 2003 Elsevier Ltd. All rights reserved.

1. Introduction

The world of endohedral fullerenes [1] comprises a large variety of structures. Endohedral fullerenes like La@C₈₂ with metal ions included in the carbon cage which can be treated as a special type of a closed intercalation compound, as there exists an electron transfer from the included metals to the carbon shell. The charge distribution was found to be La⁺@C₈₂⁻. Besides these monometal fullerenes which have been isolated as the first endohedral structures [1], there exists a larger number of di- and trimetal structures in fullerene cages. Among these multimetallofullerenes, the Sc₃@C₈₂ structure is a very important one as the three metal ions can be shown by ESR spectroscopy to be completely equivalent in the position and state at room temperature [2]. The position of the scandium ions inside the cage can be changed at lower temperatures as detected by ESR spectroscopy [2]. This change of the incorporated metal ion position is very important in comparison to a new class of fullerenes: the nitride cluster fullerenes of the general formula M₃N@C₂ₙ, first introduced in 1999 [3]. These

cluster fullerenes as a new type of endohedral fullerenes embraces an encaged trimetal nitride cluster structure, which is not stable as a single molecule. On the other hand, the carbon cages of Sc₃N@C₆₈, Sc₃N@C₇₈ and Sc₃N@C₈₀ has not been isolated as empty cages so far. Apparently these cage isomers are stabilised by the interaction with the nitride cluster [4]. The stabilising effect of the nitride cluster is a further subject of detailed studies on the nitride cluster fullerenes to understand why such fullerenes are stabilised in two ways: by the action of the carbon cage and by the covalent bonds of the cluster to the cage.

Unfortunately endohedral fullerene structures described in the past were synthesised at very small yields. Generally endohedral metallofullerenes are found in a yield of 2% or less in the fullerene soot. This causes tremendous problems in the isolation of endohedral fullerenes. There was already some indication in the first description of the Sc₃N@C₈₀ fullerene formation that there seems to be a higher abundance of this cluster fullerene in the soot extract ranging from 3 to 5% [3]. Nevertheless, there is still a strong demand to improve the yield of the endohedral fullerenes to open fields of application for these structures. While in the first study, air traces were used as a source of nitrogen, an improved route for nitride cluster formation has to search

for other selective nitrogen sources. After a first indication of an improved yield of $Sc_3N@C_{80}$ [5], more detailed studies have been undertaken which are presented here.

Because of the crucial role of the nitride cluster for the fullerene stability [4], a variety of $M_3N@C_{80}$ structures with uniform and mixed metal clusters have been produced and isolated, where $M = Y$, Tb, Ho, Tb and Er. FTIR spectroscopy was used to check the preference of the I_h-C_{80} isomer for trimetal nitride inclusion. Moreover, the role of the trimetal nitride cluster composition for the abundance and stability of trimetal nitride cluster fullerenes was studied.

Finally, the onset of Vis/NIR absorption of trimetal nitride C_{80} cluster fullerenes was studied to decide whether all nitride cluster fullerenes under study have no NIR absorptions and do not behave like low band-gap materials as it is the case for $Sc_3N@C_{80}$ [5]. $La_2@C_{80}$ and C_{60} were included for comparison to the nitride cluster fullerenes.

2. Experimental

The Krätschmer–Huffman arc burning method was used for the production of the fullerene soot. In general, graphite rods filled with a metal/graphite or metal oxide/graphite powder mixture were applied. The nitride cluster fullerenes have been prepared in two different modifications of this process. In a first version of the process, a solid nitrogen source was used by adding amounts of calciumcyanamide to the metal/graphite powder mixture. As the main synthetic route, the concept of the reactive arc atmosphere [6] was applied to improve the ratio of trimetal nitride fullerenes to empty fullerenes what is described in the results section.

The soot of the arc burning process was first pre-extracted with acetone for several hours to remove non-fullerene products like polycyclic aromatic hydrocarbons (PAH) and other low molecular structures. Subsequently the fullerenes were soxhlet extracted by CS_2 for 20 h.

High performance liquid chromatography (HPLC) was used for fullerene purification. Due to the high content of the $M_3N@C_{80}$ structures, they have been isolated by a single separation step using a 4.6 × 250 BuckyPrep column (Nacalai Tesque) to get samples of a purity >95%. Mixed metal clusters like $Er_xSc_{3-x}N@C_{80}$ ($x = 1, 2$) were separated in three steps using a linear combination of three analytical BuckyPrep columns.

The mass spectrometric characterisation was done by MALDI-TOF mass spectrometry using the Biflex II spectrometer (Bruker, Germany) and 9-nitroanthracene as the matrix. The positive and negative ions of the fullerenes have been detected.

UV–Vis–NIR spectra of the purified fullerene samples were preferably measured in toluene solution using an UV 3101 PC spectrometer (Shimadzu, Japan) in suprasil 300 quartz cells of 10 mm path length in the range of 200–2000 nm with a resolution of 2 nm.

For FTIR spectroscopic measurements, solutions of 20–200 μg fullerene in toluene were used to dropcoat KBr single crystal disks. Residing solvent was removed by heating the polycrystalline films in a vacuum of 10^{-6} mbar at 250 °C for 4 h. FTIR spectra were recorded at room temperature by an IFS 66 V spectrometer (Bruker, Germany).

3. Fullerene formation

The production of the nitride cluster fullerenes by the Krätschmer–Huffman method was done in two different ways. In a first stage, a solid nitrogen containing compound was applied which does not contain oxygen. The choice was calciumcyanamide, which was added to the metal oxide/graphite powder mixture. For all preparations, a carbon/metal ratio of 12.5 was used for the production of the fullerene soot. The addition of calciumcyanamide to the same extent as the metal content in the mixture was applied for cluster fullerene preparation. The reaction scheme for solid state reaction is:
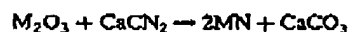
$$M_2O_3 + CaCN_2 \rightarrow 2MN + CaCO_3$$

$$3MN + 2C \rightarrow [M_3N]^\oplus + (CN)_2$$

where the bracket $[XX]^\oplus$ points to a structure which is only stable as an endohedral one in a carbon cage. It is obvious that a side reaction can occur according to

$$CaCN_2 + C \rightarrow CaC_2 + N_2$$
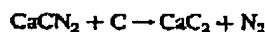
what results in gaseous nitrogen as used in Ref. [3] but in our case, without any amount of oxygen. During the arc burning process, there was an increase of the pressure of the helium atmosphere pointing to the formation of gaseous nitrogen.

The soot produced with the above given composition (Sc as the metal) of the graphite rods was extracted by CS_2 for 20 h and analysed by HPLC at the BuckyPrep column. The result is shown in Fig. 1 for the scandiumnitride fullerenes, where the fractions are analysed by mass spectrometry. In this way, the endohedral $Sc_3N@C_{80}$ is the main product of the fullerene soot. Besides $Sc_3N@C_{80}$, a further endohedral structure $Sc_3N@C_{78}$ is produced in a sufficient amount to be separated by HPLC. The fullerenes C_{60} and C_{70} which were up till now in all arc burning processes, the main component of the soot appear to be the byproducts of the reaction.

The $Sc_3N@C_{80}$ fullerene samples were preferably formed with a selectivity ranging from 3 to 42%. The yields were in each case determined from the area of the HPLC peaks. For the higher values, this is an improvement of the nitride cluster yield by a factor of 10. It is obvious that the new nitrogen source causes strong increase of the selectivity of the endohedral nitride cluster fullerene. The disadvantage of the new fullerene production was the low reproducibility of the fullerene yield. The reason for the variation of the selectivity is not clear but traces of water
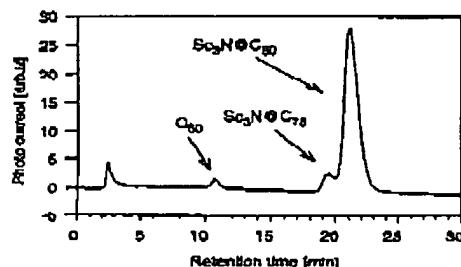
311

Fig. 1. HPLC of a $Sc_3N@C_{2n}$ soot at a Buckyprep column with toluene as an eluent.

and/or hydrocarbons were expected to be the reason. Therefore, the concept of the reactive gas atmosphere was developed which was studied in more detail.

The trimetal clusters in endohedral fullerenes were assigned to be a derivative of ammonia as a simple nitrogen compound. Therefore, nitrogen should be available in the prestabilised form to end up in the trimetal nitride state by substitution of the hydrogen in ammonia.

Furthermore, ammonia as a gas should be available for the reaction in the arc of the Krätschmer–Huffman method together with the cooling gas what seems to be preferable for the production of the nitride cluster fullerene. The formation of the cluster fullerenes by the addition of 10–20 mbar of ammonia to 200 mbar of helium as the cooling gas results in a completely new condition of fullerene production.

As shown in Fig. 2, the reactive cooling gas with ammonia as a reactive component causes a complete transformation of the ammonia as concluded from the absence of the ammonia line in the Raman spectrum at around 3340 cm^{-1} at the end of the arc burning. Thus, ammonia takes part in the chemical reactions in the arc burning process while molecular nitrogen is still present
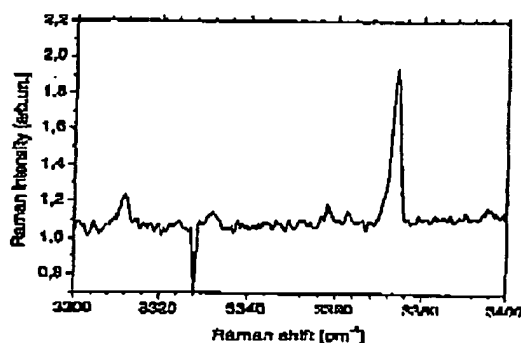

Fig. 2. Raman spectrum of the cooling gas containing ammonia for the production of $M_3N@C_{80}$ fullerenes. As seen by the pattern in the range of 3330–3340 cm^{-1}, there is no ammonia to be detected after the arc burning process.
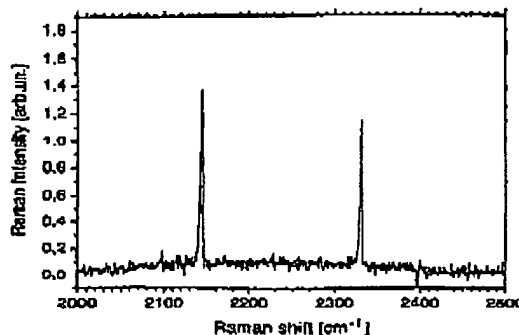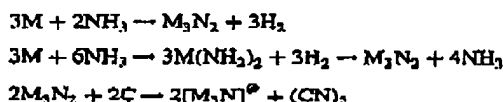

Fig. 3. Raman spectrum of the cooling gas containing nitrogen for the production of $M_3N@C_{80}$ fullerenes. As seen by the pattern at 2330 cm^{-1}, there is still a large amount of non-reacted nitrogen.

after arc burning as the vibrational spectrum of the reactor demonstrates (see Fig. 3).

The addition of ammonia to the cooling gas and using a metal oxide/graphite powder mixture for cluster fullerene preparation gives rise of a reaction mechanism for the gas phase:

$$3M + 2NH_3 \rightarrow M_3N_2 + 3H_2$$

$$3M + 6NH_3 \rightarrow 3M(NH_2)_2 + 3H_2 \rightarrow M_3N_2 + 4NH_3$$

$$2M_3N_2 + 2C \rightarrow 2[M_3N]^{\oplus} + (CN)_2$$

where the bracket [XX]$^{\oplus}$ points to a structure which is only stable as an endohedral one in a carbon cage. The dicyano is unstable at the temperature of arc burning to form by reaction with hydrogen a certain amount of HCN. It is obvious that the hydrogen is preferably reacting with carbon according to

$$MC_2 + 2H_2 \rightarrow M + C_2H_2$$
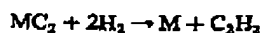
what results finally in formation of polycyclic aromatic hydrocarbons and other low molecular hydrocarbons as byproducts which are easily to be washed out by acetone from the soot. During the arc burning process, all non-gaseous products are deposited at the cooled wall of the arc burning apparatus.

The soot produced with the above given composition of the cooling gas was extracted by CS_2 for 20 h and analysed by HPLC at the BuckyPrep column in a single step. As shown in Fig. 4 for the holmiumnitride fullerenes, the endohedral $Ho_3N@C_{80}$ is the main product of the fullerene soot like $Sc_3N@C_{80}$ in the first example. With the reactive gas atmosphere, the endohedral structure $Ho_3N@C_{80}$ is produced in a selectivity up to 60% as determined by HPLC. The reproducibility is in the range of ±20%. The empty fullerenes C_{60} and C_{70} are the byproduct of the reaction of the arc burning process. With the procedure given, endohedral fullerenes can be the main component of the fullerene soot and a selectivity of up to 90% (Sc fullerene)
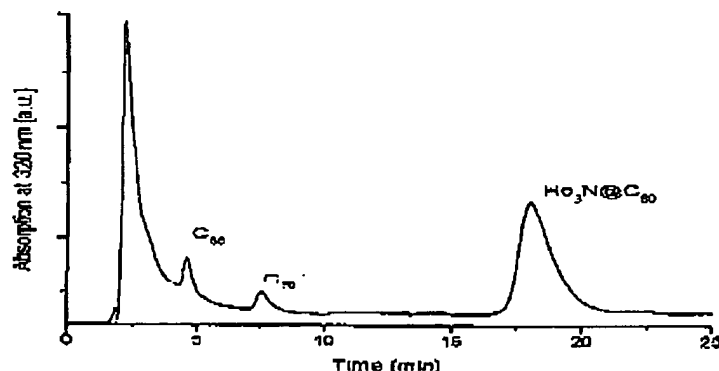
312

Fig. 4. HPLC of a Ho₃N@C₂ₙ, soot at a Buckyprep column with toluene as an eluent.

for the endohedral C₈₀ structure can be reached what is demonstrated for the first time.

4. FTIR spectroscopy: cage isomer identification and trimetal nitride cluster structural analysis

As for fullerenes, in general, the determination of the cage isomer is one of the main subjects of the structural analysis for nitride cluster fullerenes. The manifold of isomers arises from the different possibilities to arrange pentagon and hexagon rings on a closed carbon shell for a given number of atoms. While for the smallest fullerene molecule C₂₀ as well as the next smallest C₂₄ and C₂₆, only one possibility for the formation of a carbon cage exists, with the C₂₈ cages, the number of fullerene isomers becomes quickly very large. It is approaching 1812 for the 12 pentagons and 20 hexagons of C₆₀ [7]. In the experiment, however, only one C₆₀ isomer is observed. It has icosahedral symmetry and all 12 pentagon rings are separated from each other by the 20 hexagons. This structural principle is termed isolated pentagon rule (IPR). It is of general validity for unfilled fullerenes. The IPR has its physical origin in the lower stability of eight π electron systems which are formed by pentagon fusing. For endohedral fullerenes, however, pentagon adjacencies can be stabilized by the charge transfer of two electrons from the encaged species to the fullerene. A violation of the IPR has been observed for Sc₂@C₆₆ and the nitride cluster fullerene Sc₃N@C₆₈ [8,9]. However, it should be noted, that these non-IPR structures were formed with much lower abundance than endohedral fullerenes obeying the stability rule.

Infrared spectroscopy has been proven as a powerful tool for structural analysis of fullerenes. Experimental evidence for the Iₕ symmetry of C₆₀ was first obtained by the number of four lines in the FTIR spectrum, which are expected from

vibrational selection rules [10]. The proof for the Iₕ cage isomer of Sc₃N@C₈₀ was provided by the ¹³C NMR spectrum, which showed two lines with an intensity ratio of 3:1 according to the number and abundance of symmetry independent carbons [3,11]. The analysis of the infrared spectra of Sc₃N@C₈₀ and Y₃N@C₈₀ revealed more than the six allowed Iₕ-C₈₀ lines. The origin of this observation is a dynamical distortion of the Iₕ symmetry, as the trimetal nitride cluster diffuses inside the carbon cage via bonded M₃N-C₈₀ states of C₃ᵥ local symmetry [4]. Nevertheless, the number of infrared active lines was much lower than for other empty and endohedral fullerenes and is characteristic for a highly symmetric C₈₀ cage [12,13].

In Fig. 5, the mid infrared spectra of six trimetal nitride fullerenes and La₂@C₈₀ are shown in comparison to a calculated spectrum of Iₕ-C₈₀ [14]. The tangential cage mode range is dominated by a very strong, split line group around 1380 cm⁻¹. Three medium intense line groups appeared around 1515, 1450, and 1200 cm⁻¹. Due to the small number of infrared lines and the general agreement of the vibrational structure, Tb₃N@C₈₀, Ho₃N@C₈₀, ErSc₂N@C₈₀, Er₂ScN@C₈₀, and Er₃N@C₈₀ are assigned to the Iₕ-C₈₀ cage isomer as it was previously established for La₂@C₈₀ and Sc₃N@C₈₀ [3,15].

At lower energies, the trimetal nitride fullerenes exhibit a very strong, metal-dependent absorption, which is absent for La₂@C₈₀ (Fig. 5, left). Due to its metal dependence and supported by quantumchemical calculations for Sc₃N@C₈₀ this line is assigned to the antisymmetric metal-nitrogen stretching vibration—νₐₛ (MN)—of the M₃N cluster [4]. For a trigonal planar four atomic molecule, this mode is doubly degenerated and one line should appear in the spectrum. This has been observed for Sc₃N@C₈₀. For the other cluster fullerenes, νₐₛ (MN) is split into two components, indicating a distortion of the trigonal geometry. Explicit spectroscopic data are listed in Table 1. The largest splitting of 64 cm⁻¹ was observed for the mixed metal cluster
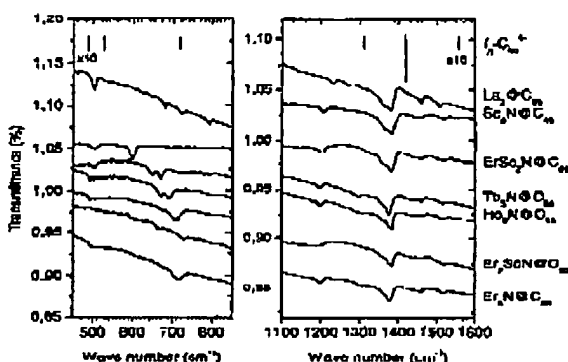
313

Fig. 5. Mid infrared spectra of $La_2@C_{80}$ and various $L_xM_{3-x}N@C_{80}$: 500 accumulations. 2.0 cm^{-1} resolution; spectra were shifted along intensity axis for representation; a calculated FTIR spectrum of C_{80}^{6-} taken from Ref. [9] is included in form of vertical bars.

fullerene $Er_2ScN@C_{80}$. Intermediate splitting energies of 20 cm^{-1} were found for the mixed metal cluster fullerene $ErSc_2N@C_{80}$ and for $Tb_3N@C_{80}$. Interestingly, terbium has the largest ionic radius of the metals under study as listed in Table 2. Small splittings in the order of 10 cm^{-1} or less were observed for Y_3N, Ho_3N and Er_3N inside I_h-C_{80} and for Sc_3N encaged in the smaller C_{78} fullerene. Thus, our analysis revealed the following quantities of influence on the ν_{as} (MN) line splitting:

(i)   the presence of different metals,
(ii)   the ionic radius,
(iii) the fullerene cage.

The frequency of ν_{as} (MN) attributed to the metal nitrogen vibrations allows further conclusions on the structure of the trimetal nitride cluster. For identical, trigonal planar valence force fields the frequency should depend on

Table 1
Spectroscopic data of the antisymmetric metal–nitrogen vibration in $L_xM_{3-x}N@C_{80}$ ($0 \leq x \leq 3$); intensity labels as usual

Sample	Wave numbers (cm^{-1})	Splitting energies (cm^{-1})
$Sc_3N@C_{80}$	599 vs	0
$Sc_3N@C_{78}$ (data from Ref. [11])	622 vs, 629 vs	7
$ErSc_2N@C_{80}$	647 vs, 667 vs	20
$Tb_3N@C_{80}$	687 s, 689 vs	20
$Ho_3N@C_{80}$	703 vs, 711 vs	8
$Er_2ScN@C_{80}$	661 s, 725 s	64
$Er_3N@C_{80}$	704 s, 713 vs	9
$Y_3N@C_{80}$ (data from Ref. [6])	712 vs, 724 vs	12
$La_2@C_{80}$	—	—

Table 2
Ionic radii of the metals under study (M^{3+} ions, coordination number = 6), after Ref. [12]

Sc^{3+}	Y^{3+}	Tb^{3+}	Ho^{3+}	Er^{3+}
74.5 pm	90.0 pm	92.3 pm	90.1 pm	89.0 pm

the reduced mass in the following order:

$$\nu_{as}(Sc_3N) = 1.025\,\nu_{as}(Y_3N) = 1.035\,\nu_{as}(Tb_3N)$$
$$= 1.036\,\nu_{as}(Ho_3N, Er_3N) \qquad (1)$$

In the experiment, the relationship of Eq. (1) is almost fulfilled for $Y_3N@C_{80}$, $Ho_3N@C_{80}$, and $Er_3N@C_{80}$. Compared to these structures, $Tb_3N@C_{80}$ and in particular $Sc_3N@C_{80}$ have significantly lower ν_{as} (MN) frequencies. Hence, three force fields have to be taken into account for the five uniform $M_3N@C_{80}$ structures under study. This conclusion is strongly supported by the ν_{as} (MN) splitting energy ordering. The related parameters of the valence force field might be the (MN) valence force constant and the (MNM) as well as (M$_3$N) bond angles.

5. Electronic absorption spectra of nitride cluster fullerenes

Introducing nitride cluster fullerenes, their obvious low energy onset in NIR absorption was pointed out to have these nitride cluster fullerenes as low band gap materials [3]. More detailed studies in our group [5] have shown that this NIR onset is not caused by the nitride cluster fullerene itself. The energy difference between the highest occupied and the lowest unoccupied electronic state, i.e. the HOMO–LUMO
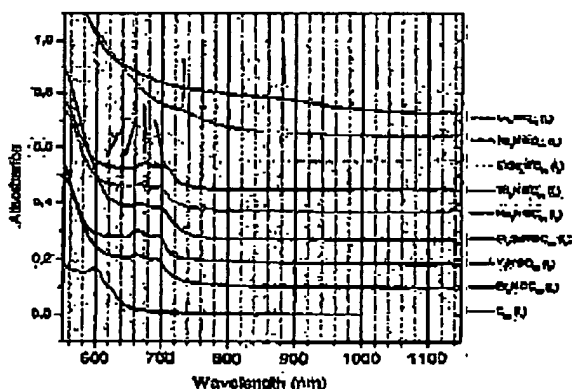

Fig. 6. Vis–NIR spectra of solutions of $La_2@C_{80}$, various $L_xM_{3-x}N@C_{80}$, and C_{60} in toluene; 2.0 nm resolution; spectra were shifted along intensity axis for representation.

314   L. Dunsch et al. / Journal of Physics and Chemistry of Solids 65 (2004) 309–315

Table 3
Vis/NIR absorptions of endohedral C_{80} fullerenes in the HOMO — LUMO region (nm (cm^{-1}))

Sample	(HOMO — LUMO)₃	(HOMO — LUMO)₄	(HOMO — LUMO)₂	(HOMO — LUMO)₁	Onset
La₂@C₈₀	–	–	770 (12,987)	880 (11,364)	1150 (8696)
Sc₃N@C₈₀	–	–	–	711 (13,605)	950 (10,526)
ErSc₂N@C₈₀	–	–	680 (14,705)	715 (13,986)	830 (11,765)
Tb₃N@C₈₀	618 (16,181)	643 (15,552)	677 (14,771)	707 (14,144)	730 (13,321)
Er₂ScN@C₈₀	602 (16,611)	631 (15,848)	670 (14,925)	702 (14,245)	800 (12,500)
Ho₃N@C₈₀	614 (16,287)	634 (15,773)	666 (15,015)	698 (14,327)	800 (12,500)
Y₃N@C₈₀	611 (16,367)	639 (15,649)	668 (14,970)	696 (14,368)	750 (13,333)
Er₃N@C₈₀	609 (16,420)	636 (15,723)	664 (15,060)	692 (14,451)	800 (12,500)
C₆₀ [16]	590.3 (16,941)	598.1 (16,720)	610.1 (16,390)	620.2 (16,124)	700 (14,286)

gap, is a crucial criterion for the electronic stability of molecular structures. It is roughly given by

$$\varepsilon_l - \varepsilon_j = \Delta E_{j \to l} + const, \qquad (2)$$

where ε_l and ε_j are the energies of the LUMO and HOMO. $\Delta E_{j \to l}$ is the observed transition energy between both states in an UV–Vis–NIR experiment and const is the sum over all contributions of the electron–electron interaction, i.e. in particular, the Coulomb interaction between the ground and excited state configuration and the exchange integral [16]. As the constant term is positive, the observed transition energy $\Delta E_{j \to l}$ is generally smaller than the HOMO–LUMO gap energy.

In Fig. 6, the Vis–NIR absorption spectra in the onset region of trimetal nitride C_{80} cluster fullerenes are compared to the response of $La_2@C_{80}$ and C_{60}. The data listed in Table 3 in wavelength and wave number units clearly demonstrate that all nitride cluster fullerenes under study have no NIR absorptions. Their spectral onsets and HOMO–LUMO transition energies are up to 0.4 eV blue-shifted in comparison to $La_2@C_{80}$. The values of $\Delta E_{j \to l} \approx 1.8$ eV for $Ho_3N@C_{80}$, $Y_3N@C_{80}$ and $Er_3N@C_{80}$ are approaching the energy of the first optical transition in C_{60} at 2 eV. Hence, all nitride cluster fullerenes under study can be assigned to the group of large band-gap fullerenes.

6. Conclusions

The concept of reactive gas atmosphere was demonstrated to cause a break through in the access to endohedral fullerenes by enlarging the selectivity of the endohedral structure production in the fullerene soot extract up to 90% of a total amount in the mg range. This is the first fullerene synthesis with an endohedral fullerene as the main fullerene product. As a consequence, the separation and purification of the nitride cluster fullerene becomes quite simple and can be managed by a single chromatographic separation. Thus, the availability of endohedral fullerenes for applied research is increased and a search for new fields of applications is facilitated.

Vis–NIR absorption spectra in the onset region of trimetal nitride C_{80} cluster fullerenes clearly demonstrate that all nitride cluster fullerenes under study have no NIR absorptions. With respect to the band-gap, they represent the most stable fullerene structures at all besides C_{60} and C_{70}.

Our results moreover point to a crucial role of the trimetal nitride cluster composition for the abundance and stability of trimetal nitride cluster fullerenes. For I_h-C_{80} structures with uniform rare earth metal nitride clusters, three quantities following the sequence $Er_3N \geq Y_3N > Ho_3N(Tb_3N$ with respect to the cluster metal were established:

(i)   the relative yield in the fullerene extract
(ii) the mass corrected frequency of ν_{as} (MN)
(iii) the transition energy of the lowest energetic electronic transition.

Similarly, the splitting energy of the antisymmetric metal–nitrogen stretching vibration, which is a measure of the cluster deformation, showed an inverse tendency. These observations indicate that steric properties of the trimetal nitride clusters have significant influence on the overall stability and formation abundance of nitride cluster fullerenes.

References

[1] For a review see:H. Shinohara, In: K.M. Kadish, R.S. Ruoff (Eds.), Fullerenes: Chemistry, Physics and Technology, Wiley, New York. 2000. p. 395.
[2] A. Bartl, L. Dunsch, Synth. Met. 121 (2001) 1147.

[3] S. Stevenson, G. Rice, T. Glass, K. Harich, F. Cromer, M.R. Jordan, J. Craft, E. Hajdu, R. Bible, M.M. Olmstead, K. Maitra, A.J. Fisher, A.L. Balch, H.C. Dorn, Nature 401 (1999) 55.

[4] M. Krause, H. Kuzmany, P. Georgi, L. Dunsch, K. Vietze, G. Seifert, J. Chem. Phys. 115 (2001) 6596.

[5] L. Dunsch, A. Bartl, P. Georgi, P. Kuran, Synth. Met. 121 (2001) 1113.

[6] L. Dunsch, P. Georgi, F. Ziegs, H. Zöller, German Patent claim, 2002.

[7] P.W. Fowler, D.E. Monolopoulos, An Atlas of Fullerenes, Clarendon Press, Oxford, 1995.

[8] Ch.-R. Wang, T. Kai, T. Tomiyama, T. Yoshida, Y. Kobayashi, E. Nishibori, M. Takata, M. Sakata, H. Shinohara, Nature 408 (2000) 426.

[9] S. Stevenson, P.W. Fowler, T. Heine, J.C. Durchamp, G. Rice, T. Glass, K. Harich, E. Hajdu, R. Bible, H.C. Dorn, Nature 408 (2000) 427.

[10] P. Georgi, Unpublished results.

[11] M. Krause, M. Hulman, H. Kuzmany, T.J.S. Dennis, M. Inakuma, H. Shinohara, J. Phys. Chem. 111 (1999) 7976.

[12] M. Krause, H. Kuzmany, in: T. Akasaka, S. Nagase (Eds.), Endofullerenes—A New Family of Carbon Clusters, Kluwer Academic Press, Dordrecht, 2002, pp. 169–183.

[13] M. Moriyama, T. Sato, A. Yabe, K. Yamamoto, K. Kobayashi, S. Nagase, T. Wakahara, T. Akasaka, Chem. Lett. (2000) 524.

[14] T. Akasaka, S. Nagase, K. Kobayashi, M. Wälchli, K. Yamamoto, H. Funasaka, M. Kako, T. Hoshino, T. Erata, Angew. Chem. 109 (1997) 1716.

[15] M. Klessinger, J. Michl, Lichtabsorption und Photochemie organischer Moleküle, VCH, Weinheim, 1989.

[16] S. Leach, M. Vervloet, A. Despres, E. Breheret, J.P. Harb, T.J. Dennis, H.W. Kroto, R. Taylor, D.R.M. Walton, Chem. Phys. 160 (1992) 451.